

Assessment of Coastal Physical Vulnerability to Climate Change Impacts along the Coast of Bolaang Mongondow Regency (North Sulawesi, Indonesia)

Hardianto Paputungan^{1*}, Rijal M. Idrus², Mahatma Lanuru³

¹ Department of Environmental Management, Graduate School, Hasanuddin University, Makassar 90245, Indonesia

² Institute of Research and Community Service, Center for Climate Change Studies, Hasanuddin University, Makassar 90245, Indonesia

³ Department of Marine Science, Faculty of Marine Science and Fisheries, Hasanuddin University, Makassar 90245, Indonesia

* Corresponding author's e-mail: hardiantopaputungan11@gmail.com

ABSTRACT

According to national climate resilience projections, the coastal area of Bolaang Mongondow has experienced an increase in wave height of around 1 meter. It is in the top priority category with high potential hazards and vulnerability or risk of climate change disasters. The rise of the global sea level affects the increase in coastal submergence and erosion and increases the frequency of overtopping of coastal buildings. This research aimed to analyze the extent of the physical vulnerability of coastal Bolaang Mongondow related to the climate change impacts. The coastal area of Bolaang Mongondow was chosen because it is a coastal area with varied lowlands that directly face the Sulawesi Sea (Pacific Ocean). The vulnerability assessment method used in this study was calculating the Coastal Vulnerability Index (CVI). Spatial data interpretation of the parameters of coastal geomorphology, elevation, coastal slope, shoreline change, sea level rise, tides, and significant wave height will contribute to the final vulnerability index value. The results showed that the weight of each analyzed variable varied, ranging from not vulnerable, moderate, vulnerable, and very vulnerable. The CVI assessment shows the less vulnerable category class in all analyzed coastal areas, with index values of 5.86 in Poigar District, 13.1 both in East Bolaang and Bolaang Districts, 14.6 in Lolak District, and 6.55 in Sangtombolang District. Thus, this research concludes that the physical condition of the Bolaang Mongondow coast is less vulnerable to the impacts of climate change. However, it is still threatened in several specific aspects. Although it has not considered socio-economic factors, the assessment of the physical vulnerability of the Bolaang Mongondow coastline produced in this study can be used to formulate targeted mitigation strategies and adaptation measures in the area.

Keywords: coastal vulnerability index, climate change impacts, Bolaang Mongondow Regency.

INTRODUCTION

The impact of climate change has become a global environmental damage phenomenon that poses serious threats to various aspects and sectors of life (IPCC, 2014). Coastal areas are no exception, as land and sea interaction areas consist of natural and social systems (Harvey et al., 2008). Global temperature changes, followed by massive sea level rise as well as an increase in the

frequency and intensity of extreme storms, threaten coastal stability (IPCC, 2023). The problem of climate change automatically becomes a danger alarm for archipelagic countries, including Indonesian coastal areas (Hecht, 2016; Suroso et al., 2011). Physical changes to the coast due to inundation and erosion as well as the increasing frequency of overtopping on coastal buildings are concrete illustrations of the direct impacts that occur (Fahmi et al., 2017; Yuliani et al., 2020).

These conditions damage infrastructure and economic assets as well as threaten natural habitats that are important for biodiversity (Bellard et al., 2012; Zlateva et al., 2024). Therefore, considering these risks, it is important to assess coastal vulnerability. Vulnerability itself is a familiar idea in relation to climate change impacts. The Intergovernmental Panel on Climate Change (IPCC) defines vulnerability as the tendency of a system to be adversely affected by climate change, including variability that depends on the type, magnitude, degree of climate variation, and the system's capacity to adapt (Denmark et al., 2001). In addition, vulnerability must be considered the opposite of disaster management resilience (Hinkel et al., 2009).

The coast of Bolaang Mongondow is an eastern part of Indonesia with a coastline length of approximately 150.79 km directly facing the Sulawesi Sea (Pacific Ocean) (BPS, 2019; Mokoginta et al., 2023). On the basis of climate change hazard studies by experts, the wave height in these waters has increased up to 1 m due to climate change and is closer to the coastal area than historical conditions, so it is necessary to increase public awareness (Bappenas, 2018). Then, in the exclusive summary document of the national climate resilience development policy, placing the Bolaang Mongondow coastal area in the top priority category, or an area that has high hazard potential with one of its high vulnerabilities or risks to the impacts of climate change (Bappenas, 2021). This argument is parallel to the characteristic conditions of the coast, which is low-lying and has striking differences in geomorphology and elevation in each area. This has led to this research hypothesis that the Bolaang Mongondow coast is vulnerable to the impacts of climate change. The hypothesis focuses on the physical components of the coast that have the potential to experience seawater inundation, erosion, and other catastrophic damage. Physical components in coastal areas are very important because they directly affect and are affected by various environmental, biological, and human processes (Cheng et al., 2022; Elko et al., 2022).

Furthermore, the hazards of climate change impacts in coastal Bolaang Mongondow have not been matched by adequate scientific research. This means that the scientific studies assessing coastal vulnerability due to the impacts of climate change are still quite limited today; most studies that show the vulnerability of these

waters are still carried out on a broad (national) scale. For example, Cintra et al. (2017) conducted the vulnerability assessment of capture fishermen due to climate change impacts by comparing coastal areas in several Indonesian provinces. Likewise, the National Development Planning Agency studied the physical vulnerability of all Indonesian coasts (Bappenas, 2018). These studies can provide a useful information baseline, but the explanatory framework is always presented more generally.

Meanwhile, localized studies are needed to provide detailed data and information for implementation at the community or specific area level (KLHK, 2017). This is still considered a gap regarding climate change issues in certain areas that needs to be bridged. Therefore, to bridge this gap and answer the hypothesis, this research aimed to assess the extent of physical vulnerability of the coastal areas of Bolaang Mongondow to the impacts of climate change. The assessment was conducted by quantitatively analyzing physical variables (coastal geomorphology, shoreline change, elevation, and coast slope) and oceanographic variables (sea level rise, tidal range, and significant wave height).

MATERIAL AND METHOD

Study area

Data collection and analysis procedures

The data used is secondary data from the digitization of satellite imagery in the last ten years (2014–2024) and obtained from credible sources (Figure 1).

Coastal geomorphology

Geomorphology was obtained through landforms from image data interpretation and direct field observations as validation. The initial process was to visit the website <https://earthexplorer.usgs.gov/> and select the location according to the study for download. The data was then pre-processed using normalized difference vegetation index (NDVI) software, which included radiometric calibration, atmospheric correction, and geometric correction. Each of these processes aims to correct pixel values for surface reflectance. Secondly, atmospheric influences such as clouds and dust particles were removed from the

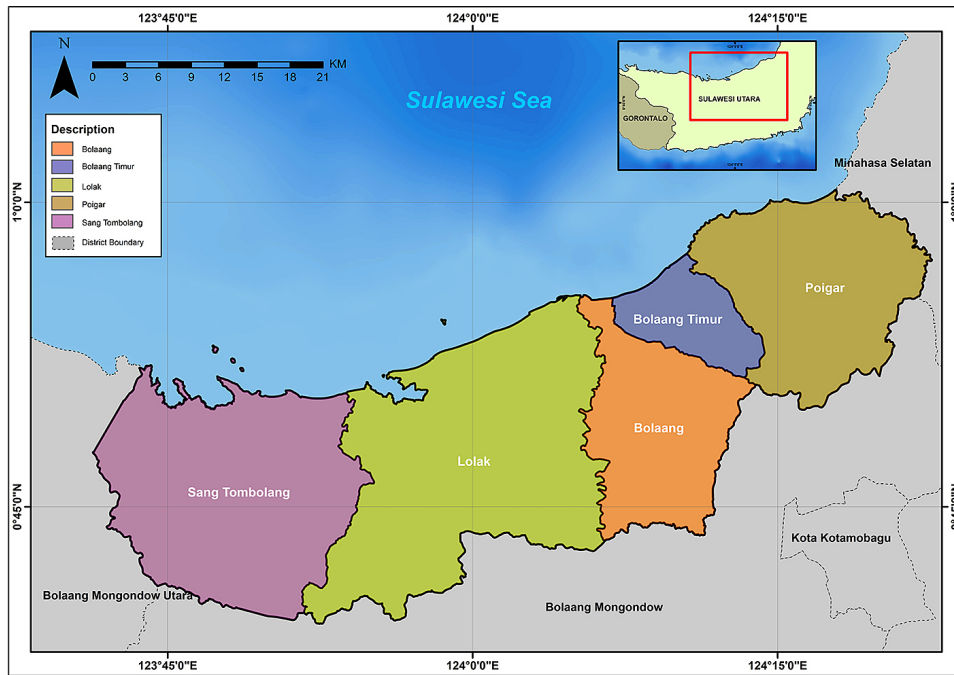


Figure 1. The research location covers five sub-districts along the coast of Bolaang Mongondow Regency. Each sub-district generally has similarities and differences in the physical characteristics of the beaches to be studied

image recording. Thirdly, the image recording was adjusted to map coordinates that match the position on the ground. Then, supervised classification was performed to identify various geomorphological features, followed by identifying landforms, such as rivers, rice fields, and hills, by looking at the patterns and colors in the image. Next, geomorphological features were extracted to separate them from vegetation using the NDVI algorithm. Digital elevation model (DEM) data and Landsat-8 imagery were combined to obtain a detailed picture of topography and landforms. Finally, a direct field review was conducted to validate the accuracy level.

Shoreline change

Shoreline changes were obtained from 2014 and 2024 Landsat-8 image data that had undergone the same correction and classification process. The image data was then used as input to determine the shoreline by digitizing each image. The digitized results were analyzed using Digital Shoreline Analysis System (DSAS) software. The initial step of DSAS is to determine the baseline that refers to the 2014 coastline. Next, transects of the same length or more were made to cover the entire shoreline, setting the transect distance of about 20 m from the baseline. The baseline shoreline length of 2024 was added, then the end point

rate (EPR) statistical calculation method was run to analyze the rate of shoreline change calculated based on two points in time (beginning and end). The statistical results will be stored in the transect attribute table and then visualized in ArcGIS to display shoreline changes in map form.

Tidal

The tides were obtained from page 10.24381/cds.6edf04e0. After previously registering and searching with the keyword ‘tidal range.’, the data download menu was selected and the filter items were filled in according to data needs. Both water level and tidal indicator variables were selected. The tidal indicator is a tidal range with absolute value-derived variables. The product type is ERA5 reanalysis and ten-year statistics. The confidence interval is the best fit, and the confidence interval is the high limit. Then, the experiment was determined by selecting historical and future. The selected period is 2015–2024. Next, the dataset was downloaded in the GeoTIFF format. The data is then rasterized and cut according to the boundaries of the study area that have been corrected previously with the extract by mask configuration in ArcGis software. Finally, zonal statistical analysis was performed to determine the comparison of data in several specified periods.

Significant wave height

The wave height data was obtained from page 10.24381/cds.adbb2d47, which results from the ERA5 reanalysis with a selected period of 2014 to 2024. The process was the same as before, with only the keywords changed to “significant wave height.” The product type selected was a reanalysis with the combined height of wind waves and significant swell variables. Next, the year, month, day, and hour were selected according to the needs of this research. Further stages are made easier by directly entering coordinates according to the research location on the web page. Then, the data set using NetCDF format was downloaded. The analysis continued in ArcGis software by importing the NetCDF data. Select significant wave variable data, adjust dimensions such as time, latitude, and longitude, and continue adding layers to the map to form a raster. Then, the data was displayed as a feature layer. The symbolization was changed to display the data informatively with color gradation. Next, the time interval was set to see significant changes in wave data over time.

Sea level rise

Sea level rise was obtained through data monitored by DUACS multimission altimetry satellite imagery for the period 2015 to 2024 via <https://doi.org/10.48670/moi-00149> and 10.24381/cds.4c328c78. Data combination was performed for temporal coverage. The original database is distributed by Aviso+ with no change in scientific content. The website provides global sea level data, so the dataset in NetCDF format had to be downloaded first, with the variable sea level height selection above sea level. The next step of data processing via ArcGIS software is the same as the previous procedure for interpreting significant wave height data.

Elevation

Coastal elevation was obtained from the National Digital Elevation Model (DEMNAS) and combined with the topography of the 1:300,000 scale Rupa Bumi Indonesia (RBI) map downloaded from <https://tanahair.indonesia.go.id/portal-web/>. After registration. The downloaded Digital Elevation Model (DEM) data had to cover the entire study site. Next, the DEMNAS data and RBI map were imported into the ArcGIS project. The topographic data of the RBI map was overlaid

on top of the DEMNAS data to find detailed location information. After that, the raster reclassification tool was used to classify the elevation values according to the specified class. The raster was converted to a polygon, elevation colors were created, and the land elevation was identified.

Beach slope

The coastal slope assessment utilized the National Bathymetry data (BATNAS) downloaded from <https://tanahair.indonesia.go.id/portal-web/>. Bathymetry is a subsurface elevation. The data was downloaded in GeoTIFF format according to the scope of the study area. The analysis process uses the buffer zone technique in ArcGis software to the sea as far as 2 km with the baseline of the 2022 coastline that has been previously digitized from Landsat-8 images. This buffer was used to evaluate the slope of the beach from the coastline. The next step was to extract bathymetry data within the buffer zone. The Clip tool in the Data Management Tools toolbox was used to cut the bathymetry data according to the buffer zone that has been created. The bathymetry layer was selected as the input raster and the buffer zone as the mask for the clip. Then, the slope was calculated using the slope tool in the spatial analyst tools toolbox. The raster from the clip was selected as the input raster. Then, the Zonal Statistics tool was used to calculate slope statistics for each buffer zone. The buffer zone was selected as the zone data input and the slope raster as the value raster input. The beach slope results were visualized with a map showing the buffer zone and slope distribution.

After all the variables were analyzed, the actual values obtained were classified on the vulnerability scoring scale formulated by Gornitz et al. (1997) and Pendleton et al. (2010) (Table 1).

Scoring values were then calculated using the CVI formula (Gornitz et al., 1994) (Equation 1). CVI is calculated as the square root of the ranked variables divided by the total number of variables. The index value indicates the coastal response to the sum of these variables.

$$CVI = \sqrt{\frac{a \times b \times c \times d \times e \times f \times g}{7}} \quad (1)$$

where: *CVI*, *a* – geomorphology, *b* – rate of shoreline change (m/year), *c* = land elevation (m), *d* – coastal slope (%), *e* – sea level rise (mm/year), *f* – average tidal ridge (m) and *g* – wave height (m).

Table 1. Scale and weight of CVI variable score

No.	Variables	Not vulnerable (score 1)	Less vulnerable (score 2)	Medium (score 3)	Vulnerable (score 4)	Highly vulnerable (score 5)
1.	Geomorphology	High cliffs	Moderate cliffs and indented shores	Low cliffs, alluvial land	Coastal buildings, beaches, estuaries and lagoons	Coastal barriers, sandy beaches, mudflats, mangroves and deltas.
2.	Shoreline change (m/yr)	> 2.0 (Accretion)	1.0–2.0 (Accretion)	+1.0 to –1.0 (Stable)	–1.1 to –2.0 (Abrasion)	≤ –2.0 (Abrasion)
3.	Elevation (m)	> 30	20.1–30	10.1–20	5.1–10	0–0.5
4.	Coastal slope (%)	> 2	1.3–1.9	0.9–1.3	0.6–0.9	< 0.6
5.	Relative sea level rise (mm/yr)	< 1.8	1.8–2.5	2.5–3.0	3.0–3.4	> 3.4
6.	Tidal (m)	< 1.0	1.0–2.0	2.0–4.0	4.0–6.0	> 6.0
7.	Wave height (m)	< 0.55	0.55–0.85	0.85–1.05	1.05–1.25	> 1.25

Furthermore, the results of the calculation of the Bolaang Mongondow coastal vulnerability index are classified based on the vulnerability class category (Table 2) according to the formulation of Hammar-Klose et al. (2003) and Suhana et al. (2017).

RESULTS AND DISCUSSION

On the basis of the results of direct surveys and interpretation of satellite data, the value of each variable had a fairly varied level of vulnerability in each sub-district, ranging from the category of not vulnerable to very vulnerable (Table 3).

Table 2. Coastal vulnerability class categories

CVI value	Vulnerability class
0.38–4.28	Not vulnerable
4.29–17.68	Less vulnerable
17.69–48.38	Medium
48.39–105.63	Vulnerable
105.64	Highly vulnerable

Furthermore, these findings are discussed in this study, especially how each variable intersects with the impact of climate change itself.

Geomorphological vulnerability

To validate accuracy, coastal geomorphology was determined using remote sensing data and direct observation. The conducted analysis found that the coastal characteristics of Bolaang Mongondow Regency are dominated by sandy beaches in all sub-districts. There are also estuaries, more residential areas in three sub-districts (Poigar, East Bolaang, and Bolaang), as well as mangrove vegetation and coral reefs in only two sub-districts (Lolak and Sangtombolang). According to Supriyadi et al. (2019), who conducted vulnerability research on the coast of Bintan, Riau Islands, argue that sandy beaches with sloping land and hills have a risk of erosion by weathered rocks and cause the land to be covered with more sediment deposits. As there are geological variations at each station, assessment of this variable was focused on the tendency of sandy, gently sloping beaches and the presence

Table 3. Vulnerability variables scoring results

Subdistrict name	Weight score vulnerability (variable)						
	Geomophology	Shoreline change	Elevation	Beach slope	Sea level rise	Tidal	Significant wave height
Poigar	4 (vulnerable)	5 (highly vulnerable)	1 (not vulnerable)	1 (not vulnerable)	1 (not vulnerable)	3 (medium)	4 (vulnerable)
Bolaang timur	4 (vulnerable)	5 (highly vulnerable)	5 (highly vulnerable)	1 (not vulnerable)	1 (not vulnerable)	3 (medium)	4 (vulnerable)
Bolaang	4 (vulnerable)	5 (highly vulnerable)	5 (highly vulnerable)	1 (not vulnerable)	1 (not vulnerable)	3 (medium)	4 (vulnerable)
Lolak	5 (highly vulnerable)	5 (highly vulnerable)	5 (highly vulnerable)	1 (not vulnerable)	1 (not vulnerable)	3 (medium)	4 (vulnerable)
Sangtombolang	5 (highly vulnerable)	5 (highly vulnerable)	1 (not vulnerable)	1 (not vulnerable)	1 (not vulnerable)	3 (medium)	4 (vulnerable)

of coral reef areas and mangrove vegetation characterized by muddy substrates. Therefore, the coast of Bolaang Mongondow Regency is categorized as Vulnerable and Highly Vulnerable – the description of coastal geomorphology in Table 4. In addition, researchers also found high cliff land in Poigar and Sangtombolang sub-districts. However, it is still quite risky because the land type is alluvial, as seen from the presence of sewahs and community ponds at points. Alluvial plains make an area prone to climate change disasters such as abrasion, accretion, and coastal erosion. (Huda et al., 2019).

Shoreline vulnerability

Changes in the coastal shoreline of Bolaang Mongondow Regency experience significant dynamics. The results of the Digital Shoreline Analysis System from Landsat image data from 2014 to 2024 show that the distance of shoreline change is included in the very vulnerable class.

Table 5 shows that the weighted vulnerability value of shoreline change is well below minus 2.0 m/year. In other words, all of Bolaang Mongondow’s coastal sub-districts have experienced abrasion in the last ten years. The largest abrasion occurred in East Bolaang, and the lowest was in Sangtombolang. This condition cannot be separated from the impact of climate change, such as tides, increased waves, and storms that continuously erode coastal land (Lyddon et al., 2019; Sanford et al., 2017). This positively correlates with the results of coastal geomorphology, tidal, and wave height studies, which are quite influential in the study area. In addition, some damage to tourism infrastructure and residential housing found in the field is a strong indication of vulnerability due to changes, although anthropogenic factors may contribute in this context.

Elevation vulnerability

DEMNAS data was used in the elevation analysis, which is data on land height above sea

level. The results of the conversion of analog mapping data show that the elevation conditions of the Bolaang Mongondow coast are on a scale of not vulnerable and very vulnerable. The values obtained are in the range of 1.65 to > 30 m. The land position that is quite sloping on the land surface is in the sub-districts of Bolaang, East Bolaang, and Lolak, with elevations that are below average. Although Poigar and Sangtombolang sub-districts have some sloping land, they have hilly cliffs that lead directly to the coastal area and form a barrier between beaches. This theoretically has the potential to experience erosion threats but is still translated as not vulnerable, because it tends to experience a greater reduction in wave energy before reaching land (Davidson et al., 2019; Supriyadi et al., 2019). The elevation level ratio can be seen in Table 6.

Calculating the elevation of coastal areas is very important in estimating their vulnerability, because the potential impact of the advance and retreat of the coastline due to climate change depends on the elevation of the land area. When there is a tidal wave, the beach with a high elevation will prevent water from entering the land; otherwise, if

Table 4. Coastal geomorphology characteristics of Bolaang Mongondow

No.	Subdistrict name	Geomorphology
1.	Poigar	Beach building, sandy beach, estuary, alluvial
2.	Bolaang Timur	Beach building, sandy beach
3.	Bolaang	Beach building, sandy beach, estuary
4.	Lolak	Beach buildings, sandy beaches, mangrove vegetation, coral reefs
5.	Sangtombolang	Beach building, sandy beach, mangrove vegetation, coral reef, alluvial plain

Table 5. Shoreline change rate in 2014 and 2024

No.	Subdistrict name	Shoreline change (m/year)
1.	Poigar	-39.7
2.	Bolaang Timur	-100
3.	Bolaang	-97.3
4.	Lolak	-67.4
5.	Sangtombolang	-31.1

Table 6. Coastal elevation of Bolaang Mongondow

No.	Subdistrict name	Elevation (m)
1.	Poigar	> 30
2.	Bolaang timur	1.78
3.	Bolaang	1.65
4.	Lolak	3.98
5.	Sangtombolang	> 30

the elevation is low, it will cause water to enter the land with the risk of extensive overflow (Marwasta et al., 2016). In addition, it is important to note that regardless of the land cover in the coastal area, the lower elevations of land remain vulnerable to inundation by seawater (Hamuna et al., 2019).

Coastal slope vulnerability

The coastal slope level of the Bolaang Mongondow coast is the data from the bathymetry contour map or the slope of the water bottom slope, which is approximately 2 km from the coastline. The analysis results obtained a slope value of more than 2% or in the percentage range of 2.56–4.31% at all sub-district points. This means that the Bolaang Mongondow coastal area has a slope that is not steep below sea level and is not sufficiently risky to coastal dynamics. The physical parameter of the coastal slope is very important as data for coastal vulnerability research and climate change hazards. This is because low-slope beaches have the potential for shoreline retreat or accretion due to tidal fluctuations and wave activity (Boruff et al., 2005; Handartoputra et al., 2015). This is briefly related to the results of the analysis of changes in the coastline experiencing abrasion. The level of the coastal slope is presented in Table 7.

Table 7. Beach slope

No.	Subdistrict name	Beach slope (%)
1.	Poigar	4.31
2.	Bolaang Timur	4.27
3.	Bolaang	2.56
4.	Lolak	2.98
5.	Sangtombolang	2.91

Relative sea level rise vulnerability

Sea level rise along the Bolaang Mongondow coast was obtained through altimetry satellite imagery data available from 1993, while the data used was only from 2015 to 2024. The relative surface rise value obtained is 0.071–0.073 mm/year or in the non-vulnerable category (Figure 2a). This value is obtained from considering local land activities such as subsidence or uplift. However, despite the non-vulnerable status, Topex/Poseidon altimetry satellite monitoring data in this area shows a periodic annual rise in sea level (MSL) of 0.051–0.096 mm/year (Figure 2b). The vulnerability status of this study generally applies at the local scale, while national projections through several scenarios suggest Indonesia’s coastal position will be highly vulnerable in the future (ICCSR, 2010b; Vinata et al., 2023). Sea level rise is a major risk and indicator of climate change. According to the Intergovernmental

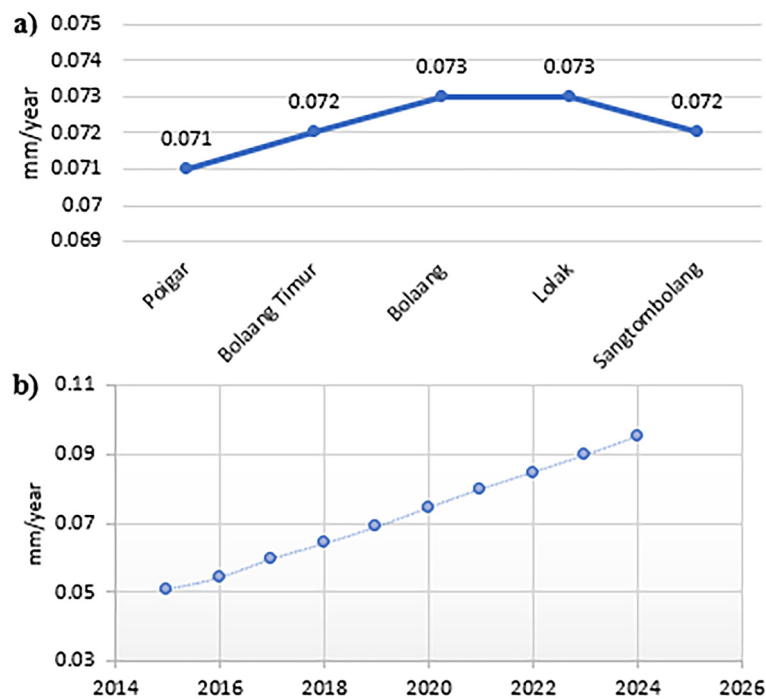


Figure 2. a) Relative water level rise b) Average yearly sea level rise. Generated using E.U. Copernicus marine service information; <https://doi.org/10.48670/moi-00149>

Panel on Climate Change (IPCC) study in the Fourth Assessment Report document, there are at least two main causes of sea level rise: the increase by thermal expansion of seawater due to rising sea temperatures and the increase due to the melting of polar ice caps and other areas that can increase the volume of seawater. (Mackay, 2008).

Tidal

Determination of the coastal vulnerability index with tidal parameters generally uses the tidal range value obtained from the difference between the Mean Highest Water level (MHWL) and the Mean Lowest Water Level (MLWL). The average tidal range value in the coastal waters of Bolaang Mongondow is in the range of 2.14 to 2.24 m or in the medium vulnerability scale. Tidal Ridges can be seen in (Table 8). The tidal type of the Bolaang Mongondow coastal area is a mixed semi-diurnal tide. This is in line with the findings of [Lesmana et al., 2021; Mulyabakti et al., 2016], considering the proximity of the study area that covers the waters of North Sulawesi. Tidal criteria and type as a climate change variable correlate with coastal vulnerability because they indicate sediment transport and erosion (Georgiou et al., 2024). On the basis of these findings, it is not an exaggeration to say that the occurrence of significant shoreline changes in the Bolaang Mongondow coastal area has a large contribution from the tides that occur.

Significant wave height vulnerability

The results of the ERA5 reanalysis of significant wave heights on the coast of Bolaang Mongondow Regency are grouped in the vulnerable class. The range of values for each sub-district is 1.13–1.15 m, with the highest wave dynamics occurring in Poigar and East Bolaang and the lowest in Sangtombolang (Table 9). Being directly facing the Sulawesi Sea, the results of this study intersect with the study of Molle et al. (2022) in

Table 9. Significant wave height

No.	Subdistrict name	Significant wave height (m)
1.	Poigar	1.13
2.	Bolaang Timur	1.13
3.	Bolaang	1.14
4.	Lolak	1.13
5.	Sangtombolang	1.15

the waters of Bunaken Island, Mantehage, and Nain Island, North Sulawesi, with significant wave height findings in the range of mild to high criteria. This is not separated from the influence of climatic activities in the Pacific Ocean. High wave intensity is strongly influenced by changes in air circulation (direction and speed), because the wind supplies energy in wave activity, the greater the wind strength or in the size of the storm, the greater the wave intensity (Yuliani et al., 2020). In addition, according to Benkhattab et al. (2020), the storm surge phenomenon increases the vulnerability of the coastline with the threat of abrasion and its destructive impact when a disaster occurs. This is quite consistent with estimating the variable of shoreline change in this coastal area, which is experiencing abrasion.

Coastal vulnerability index of Bolaang Mongondow Regency

On the basis of the results of the analysis, the highest vulnerability index value is in Lolak Sub-district with CVI = 14.6, followed by Bolaang and East Bolaang, respectively, with the same value of CVI = 13.1, and the lowest in the remaining two sub-districts, namely Sangtombolang with CVI = 6.55 and Poigar with a value of CVI = 5.86. Thus, overall, the coastal areas of Bolaang Mongondow are categorized as less vulnerable to climate change risks (Table 10). The same category class with different CVI values here is a general description of the level of risk variation faced. This finding also confirms the not-so-deep difference

Table 8. Coastal tidal ridges of Bolaang Mongondow Regency 2015–2024

District	2015	2016	2017	2018	2019	2020	2021	2022	2023	2024
Poigar	2.18	2.16	2.17	2.20	2.21	2.19	2.21	2.23	2.24	2.23
Bolaang Timur	2.19	2.17	2.17	2.20	2.21	2.19	2.20	2.23	2.24	2.22
Bolaang	2.18	2.16	2.17	2.19	2.21	2.19	2.20	2.23	2.23	2.21
Lolak	2.15	2.14	2.15	2.17	2.18	2.18	2.19	2.21	2.21	2.21
Sangtombolang	2.17	2.16	2.16	2.18	2.20	2.17	2.19	2.21	2.23	2.21

Table 10. Bolaang Mongondow Regency coastal vulnerability index

No.	Subdistrict name	CVI index	Category
1.	Poigar	5.86	Less vulnerable
2.	Bolaang Timur	13.1	Less vulnerable
3.	Bolaang	13.1	Less vulnerable
4.	Lolak	14.6	Less vulnerable
5.	Sangtombolang	6.55	Less vulnerable

with the results of the National Marine and Fisheries Research Agency’s (MMAF) study of all Indonesian coastal areas in 2010, where the coastal vulnerability index indicated on the map (specific to our research location) was in the category of not vulnerable (Bappenas, 2018; ICCSR, 2010a).

As it was previously explained, the weighting of vulnerability variables is the basis for the assessment that the less vulnerable category does

not mean any risk. Still, it has the potential for exposure to climate change impacts, specifically on specific physical components. Therefore, targeted adaptation and mitigation measures need to be pursued. While it is not possible to completely prevent natural disasters, the opportunity is there to assess and develop the solutions to reduce the destructive impacts on coastal areas. (Malehmir et al., 2016; Pratiwi et al., 2023). The physical variable vulnerability scale and coastal CVI vulnerability can be seen in Figure 3 (a, b, c, d, e, f, g, h).

CONCLUSIONS

This study succeeded in answering the research objectives and hypotheses by identifying the value of the Bolaang Mongondow coastal vulnerability index as less vulnerable to climate change impacts in all observation areas. The CVI

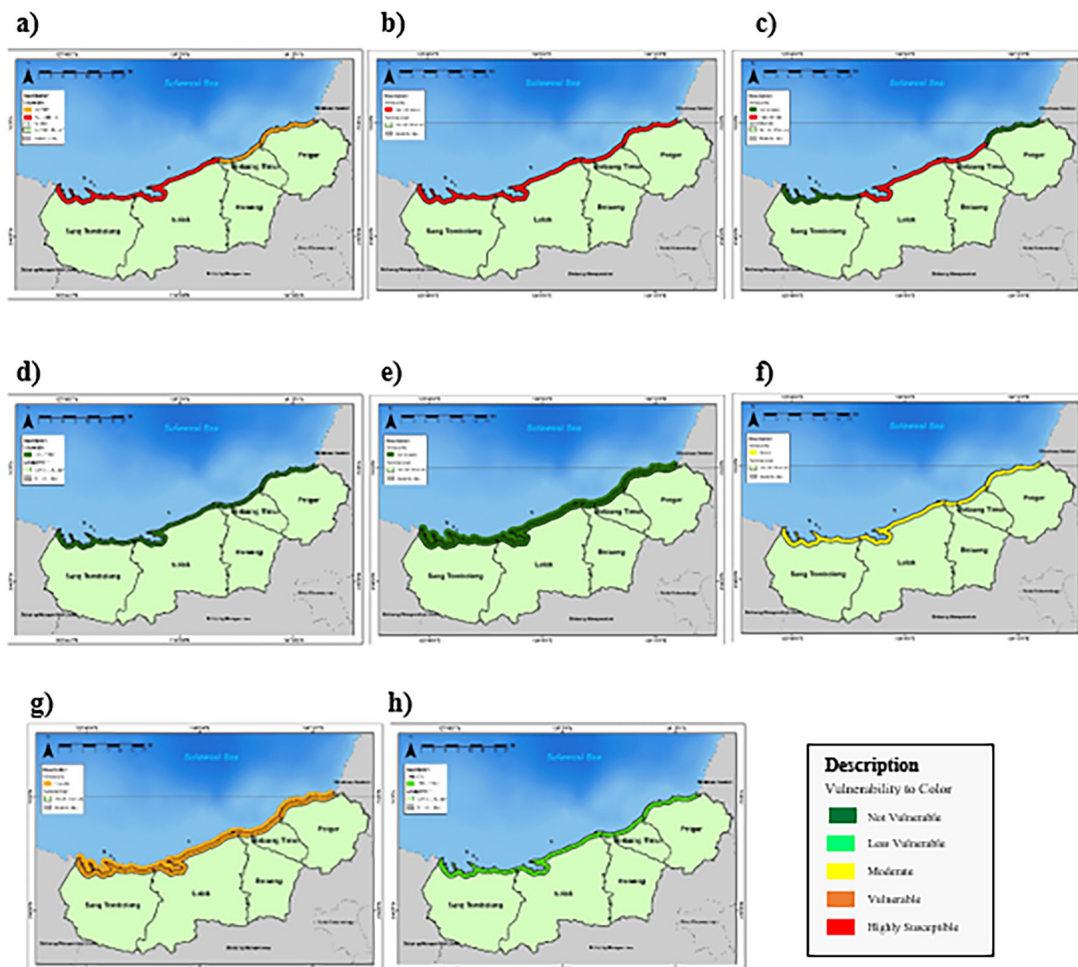


Figure 3. Vulnerability scale of physical variables and CVI vulnerability of the Bolaang Mongondow coast. The figure follows the structure of the review, (a) with maps of geomorphology, (b) shoreline change, (c) elevation, (d) coastal slope, (e) sea level rise, (f) tides, (g) significant waves, and (h) CVI vulnerability index.

values in the range of 5.86–14.6 illustrate the different levels of risk at each point as well as differences with the proposed hypothesis. This is directly influenced by coastal physical indicators that show varying scales of vulnerability. The real values of variables that are not vulnerable are coastal slope, sea level rise, and elevation. Sea tides are in moderate condition. In turn, vulnerable to highly vulnerable conditions are found in geomorphology, shoreline changes, coastal elevation, and significant waves. Thus, this scientific discovery contributes to the information gap on the vulnerability of specific local coastal areas that has never been done before. Thus, there is an opportunity to utilize the data found as a reference for targeted coastal climate change adaptation and mitigation efforts. Experts recommend coastal vulnerability studies as the first step in climate change disaster mitigation efforts at local, national and global scales.

Acknowledgments

The author would like to thank the supervisors and examiners who shared important information about this research. Then to Mr. Yasin Septian, Mr. Fajri Mamonto, and Mr. Angga Riski, who helped make maps and field survey activities, as well as the entire academic community of the Environmental Management Study Program, Hasanuddin University.

REFERENCES

1. Abuodha, P.A.O., Woodroffe, C.D. 2010. Assessing vulnerability to sea-level rise using a coastal sensitivity index: a case study from southeast Australia. *Journal of Coastal Conservation*, 14(3), 189–205. <https://doi.org/10.1007/s11852-010-0097-0>
2. National Development Planning Agency. 2018. Scientific base assessment of climate change hazards. In *National Action Plan for Climate Change Adaptation*.
3. National Development Agency. 2021. Exclusive summary: Climate Resilience Development Policy 2020-2021. 10.
4. Bellard, C., Bertelsmeier, C., Leadley, P., Thuiller, W., Courchamp, F. 2012. Impacts of climate change on the future of biodiversity. *Ecology Letters*, 15(4), 365–377. <https://doi.org/10.1111/j.1461-0248.2011.01736.x>
5. Benkhattab, F.Z., Hakkou, M., Bagdanavičiūtė, I., Mrini, A. El, Zagaoui, H., Rhinane, H., Maanan, M. 2020. Spatial-temporal analysis of the shoreline change rate using automatic computation and geospatial tools along the Tetouan coast in Morocco. *Natural Hazards*, 104(1), 519–536. <https://doi.org/10.1007/s11069-020-04179-2>
6. Boruff, B.J., Emrich, C., Cutter, S.L. 2005. Erosion hazard vulnerability of US coastal counties. *Journal of Coastal Research*, 21(5), 932–942. <https://doi.org/10.2112/04-0172.1>
7. BPS. 2019. Bolaang Mongondow Regency in Figures 02155-6431, 1–236.
8. Cheng, J., Wang, P. 2022. Factors controlling storm-induced morphology changes at an erosional hot spot on a nourished beach, Sand Key Barrier Island, West-Central Florida. *Journal of Coastal Research*, 38(4), 750–765. <https://doi.org/10.2112/JCOASTRES-D-21-00083.1>
9. Cintra, A.K.A., Setyobudiandi, I., Fahrudin, A. 2017. Analysis of fishing vulnerability against climate change on a province scale (province scaled fisheries vulnerability on climate change). *Marine Fisheries: Journal of Marine Fisheries Technology and Management*, 8(2), 223–233. <https://doi.org/10.29244/jmf.8.2.223-233>
10. Copernicus Climate Change Service, Climate Data Store, 2018: Sea level gridded data from satellite observations for the global ocean from 1993 to present. Copernicus Climate Change Service (C3S) Climate Data Store (CDS). <https://doi.org/10.24381/cds.4c328c78> (Accessed on 11-07-2024).
11. Davidson-Arnott, R., Bauer, B., Houser, C. 2019. *Introduction to coastal processes and geomorphology* (2nd ed.). Cambridge University Press. <https://doi.org/10.1017/9781108546126>
12. Denmark, C., Davidson, O., Leone, S., Uk, M.G., Denmark, K.H. 2001. Technical summary of climate change 2001: Mitigation a report of working group III of the Intergovernmental Panel on Climate Change lead authors: Review Editor: Change.
13. Elko, N., Foster, D., Kleinheinz, G., Raubenheimer, B., Brander, S., Kinzelman, J., Kritzer, J., Munroe, D., Storlazzi, C., Sutula, M., Mercer, A., Coffin, S., Fraioli, C., Ginger, L., Morrison, E., Parent-Doliner, G., Akan, C., Canestrelli, A., Dibenedetto, M., Simm, J. 2022. Human and ecosystem health in coastal systems.
14. Fahmi, R., Saleh, S.M., Isya, M. 2017. Effect of seawater soaking time on durability of concrete asphalt mixtures using pen.60/70 asphalt substituted with Ethylene Vinyl Acetate (Eva) waste. *Civil Engineering Syiah Kuala University*, 6(3), 271–282.
15. Georgiou, I. Y., FitzGerald, D.M., Hanegan, K.C. 2024. Storm and tidal interactions control sediment exchange in mixed-energy coastal systems. *Pnas Nexus*, 3(2), 42. <https://doi.org/10.1093/pnasnexus/pgae042>
16. Gornitz, V. 1991. Global coastal hazards from future sea level rise. *Palaeogeography*,

- Palaeoclimatology, Palaeoecology, 89(4), 379–398. [https://doi.org/10.1016/0031-0182\(91\)90173-O](https://doi.org/10.1016/0031-0182(91)90173-O)
17. Gornitz, V. 1997. Effects of anthropogenic interventions in the land hydrologic cycle on global sea level rise. 14, 147–161.
 18. Gornitz, V., Kanciruk, P. 1989. Assessment of global coastal hazards from sea level rise. <https://www.osti.gov/biblio/5966579>
 19. Hammar-Klose, E.S., Pendleton, E.A., Thieler, E.R., Williams, S.J. 2003. Coastal vulnerability assessment of Cape Cod National Seashore to sea-level rise. In Open-File Report. <https://doi.org/10.3133/ofr02233>
 20. Hamuna, B., Kalor, J.D., Tablaseray, V.E. 2019. The impact of tsunami on mangrove spatial change in eastern coastal of Biak Island, Indonesia. *Journal of Ecological Engineering*, 20(3), 1–6. <https://doi.org/10.12911/22998993/95094>
 21. Handartoputra, A., Purwanti, F., Hendarto Department of Aquatic Resources Management, B., Fisheries Faculty of Fisheries and Marine Science, J., Diponegoro Jl Soedarto, U. 2015. Coastal vulnerability assessment at Sendang Biru Beach, Malang Regency towards oceanography variables based on CVI (Coastal Vulnerability Index) method. *Diponegoro Journal of Maquares*, 4(1), 91–97. <http://ejournal-s1.undip.ac.id/index.php/maquares>
 22. Harvey, N., Nicholls, R. 2008. Global sea-level rise and coastal vulnerability. *Sustainability Science*, 3, 5–7. <https://doi.org/10.1007/s11625-008-0049-x>
 23. Hersbach, H., Bell, B., Berrisford, P., Biavati, G., Horányi, A., Muñoz Sabater, J., Nicolas, J., Peubey, C., Radu, R., Rozum, I., Schepers, D., Simmons, A., Soci, C., Dee, D., Thépaut, J.-N. 2023: ERA5 hourly data on single levels from 1940 to present. Copernicus Climate Change Service (C3S) Climate Data Store (CDS), <https://doi.org/10.24381/cds.ad-bb2d47> (Accessed on 11-07-2024).
 24. Hinkel, J., Klein, R.J.T. 2009. Integrating knowledge to assess coastal vulnerability to sea-level rise: The development of the DIVA tool. *Global Environmental Change*, 19(3), 384–395. <https://doi.org/https://doi.org/10.1016/j.gloenvcha.2009.03.002>
 25. Huda, A.C., Pratikto, I., Pribadi, R. 2019. Land characteristics on coastal vulnerability of Rembang Regency, Central Java. *Journal of Marine Research*, 8(3), 253–261. <https://doi.org/10.14710/jmr.v8i3.25268>
 26. ICCSR. 2010a. Iccsr. In Marine and Fisheries Sector.
 27. ICCSR. 2010b. Indonesia Climate Change Sectoral Roadmap (ICCSR). Bappenas Library, September 2016, 58.
 28. Intergovernmental Panel on Climate Change (IPCC). 2023. Oceans and coastal ecosystems and their services. In *Climate Change 2022 – Impacts, Adaptation and Vulnerability*. <https://doi.org/10.1017/9781009325844.005>
 29. IPCC. 2014. A “missing” family of classical orthogonal polynomials. *Journal of Physics A: Mathematical and Theoretical*, 44(8), 31. <https://doi.org/10.1088/1751-8113/44/8/085201>
 30. Hecht J.E. 2016. Indonesia: Costs of climate change in 2050. Usaid, May, 32. [https://www.climatelinks.org/sites/default/files/asset/document/Indonesia Costs of CC 2050 Policy Brief.pdf](https://www.climatelinks.org/sites/default/files/asset/document/Indonesia%20Costs%20of%20CC%202050%20Policy%20Brief.pdf)
 31. Kumar, T.S., Mahendra, R.S., Nayak, S., Radhakrishnan, K., Sahu, K.C. 2010. Coastal vulnerability assessment for Orissa State, East Coast of India. *Journal of Coastal Research*, 26(3), 523–534. <https://doi.org/10.2112/09-1186.1>
 32. Lesmana, N.T., Haykal, M.F. 2021. Bathymetry mapping in coastal development planning. *Journal of Empowerment Community and Education*, 1(2), 1–7.
 33. Lyddon, C., Brown, J., Leonardi, N., Plater, A. 2019. Increased coastal wave hazard generated by differential wind and wave direction in hyper-tidal estuaries. *Estuarine, Coastal and Shelf Science*, 220, 131–141. <https://doi.org/10.1016/j.ecss.2019.02.042>
 34. Mackay, A. 2008. Climate change 2007: Impacts, adaptation and vulnerability. Contribution of working group II to the fourth assessment report of the Intergovernmental Panel On Climate Change. In *Journal of Environmental Quality*, 37(6). <https://doi.org/10.2134/jeq2008.0015br>
 35. Malehmir, A., Socco, L.V., Bastani, M., Krawczyk, C., Pfaffhuber, A., Miller, R.D., Maurer, H., Frauenfelder, R., Suto, K., Bazin, S., Merz, K., Dahlin, T. 2016. Near-surface geophysical characterization of areas prone to natural hazards: a review of the current and perspective on the future. In *Advances in Geophysics* 57, 51–146. <https://doi.org/10.1016/bs.agph.2016.08.001>
 36. Marwasta, D., Priyono, K.D. 2016. Analysis of settlement characteristics of coastal villages in Kulonprogo Regency. *Forum Geography*, 21(1), 57–68. <https://doi.org/10.23917/forgeo.v21i1.1819>
 37. Mokoginta, M.P.A., Amir, A., Tanjung, I.L., Hamid, A.R. 2023. Tracing the maritime footsteps of the Bolaang Mongondow people: XVI–XIX centuries. *Gema Wiralodra*, 14(1), 137–155. <https://doi.org/10.31943/gw.v14i1.376>
 38. Molle, B., Schadu, J., Sumilat, D., Rondonuwu, A., Luasunaung, A., Warouw, V. 2022. Analysis of weather conditions and hydrodynamics in Bunaken National Park. *Platax Scientific Journal*, 10, 320. <https://doi.org/10.35800/jip.v10i2.43161>
 39. Mulyabakti, C., Jasin, M.I., Mamoto, J.D. 2016. On the Paal beach area of East Likupang District. *Journal of Civil Statics*, 4(9), 585–594.
 40. Pendleton, E.A., Thieler, E.R., Williams, S.J. 2010. Importance of coastal change variables in

- determining vulnerability to sea- and lake-level change. *Journal of Coastal Research*, 26(1), 176–183. <http://www.jstor.org/stable/27752797>
41. Pratiwi, P.H., Dwiningrum, S.I.A., Sumunar, D.R.S. 2023. Integrated disaster risk management in the education process in schools. *Journal of Integrated Disaster Risk Management*, 13(1), 172–192. <https://doi.org/10.5595/001C.91284>
42. Sanford, L., Gao, J. 2017. Influences of wave climate and sea level on shoreline erosion rates in the Maryland Chesapeake bay. *Estuaries and coasts*, 41, 1–19. <https://doi.org/10.1007/s12237-017-0257-7>
43. Muis, S., Apecechea, M.I., Álvarez, J.A., Verlaan, M., Yan, K., Dullaart, J., Aerts, J., Duong, T., Ranasinghe, R., le Bars, D., Haarsma, R., Roberts, M. 2022. Global sea level change indicators from 1950 to 2050 derived from reanalysis and high resolution CMIP6 climate projections. Copernicus Climate Change Service (C3S) Climate Data Store (CDS). <https://doi.org/10.24381/cds.6edf04e0> (Accessed on 05-07-2024)
44. Suhana, M.P., Nurjaya, I.W., Natih, N.M. 2017. Vulnerability analysis of east Coast of Bintan Island, Riau Islands Province using digital shoreline analysis system and coastal vulnerability index Method. *Journal of Fisheries and Marine Technology*, 7(1), 21–38. <https://doi.org/10.24319/jtpk.7.21-38>
45. Supriyadi, I.H., Wahyudi, A.J., Iswari, M.Y., As, S. 2019. Adaptation to the impact of climate change in coastal communities. In Indonesian Institute of Sciences (December Issue).
46. Suroso, D.S.A., Hadi, T.W., Latief, H., Riawan, E. 2011. Indonesia's coastal vulnerability patterns to climate change impacts as a basis for adaptation planning. *Journal of Tata Loka*, 13(2), 108–118.
47. Thieler, E.R., Hammar-Klose, E.S. 1999. National assessment of coastal vulnerability to sea-level rise: Preliminary results for the U.S. Atlantic Coast. In Open-File Report. <https://doi.org/10.3133/ofr99593>
48. Vinata, R.T., Kumala, M.T., Yustisia Serfiyani, C. 2023. Climate change and reconstruction of Indonesia's geographic basepoints: Reconfiguration of baselines and Indonesian Archipelagic Sea lanes. *Marine Policy*, 148, 105443. <https://doi.org/https://doi.org/10.1016/j.marpol.2022.105443>
49. Yuliani, A.D., Rejeki, H.A. 2020. The effect of waves on abrasion in the coastal Regencies of Demak, Kendal, and Semarang City. *Indonesian Journal of Oceanography*, 2(4), 378–385. <https://doi.org/10.14710/ijoce.v2i4.9290>
50. Zlateva, P., Velev, D. 2024. A vulnerability analysis of business to climate-related hazards. *IDRiM Journal*, 14, 169–180. <https://doi.org/10.5595/001c.92697>